

Image Reconstruction in 3D Short-Scan SPECT

Xiaochuan Pan, Chien-Min Kao, Charles Metz, and Alexander Kiselev*

Departments of Radiology and Mathematics*, The University of Chicago

Abstract

Physical factors such as photon attenuation degrade image quality and quantitative accuracy in single-photon emission computed tomography (SPECT). It is often considered (especially in situations with non-uniform attenuation and distance-dependent spatial resolution (DDSR)) that adequate compensation for the effects of these physical factors requires data acquired over 2π . However, as the analysis in this work suggests, one may need data acquired only over π to correct adequately for the effects of some of the physical factors. Reduction of the scanning angle in SPECT imaging is desirable because it can reduce the scanning time and thus minimize patient-motion and other artifacts, and because scans over less than 2π can allow the detector to be rotated at a fixed distance closer to the patient. Also, in certain cases (e.g., in cardiac SPECT), one can choose the scanning angular range for obtaining maximum numbers of photons. This work focuses on investigation of accurate image reconstruction in 3D SPECT from data that are acquired with parallel-beam collimation only over π and that contain the effects of photon attenuation (either uniform or non-uniform) and DDSR. For simplicity, we refer to such a scanning configuration as 3D short-scan SPECT. This work may have significant theoretical as well as practical implications for image reconstruction in SPECT.

I. BACKGROUND

Single-photon emission computed tomography (SPECT) is an important nuclear medicine imaging modality. Physical factors in SPECT such as photon attenuation and imperfect spatial resolution degrade image quality and quantitative accuracy [1, 2] and should be adequately corrected for. Because these physical factors are generally spatially variant, it is often considered (especially in the situation with non-uniform attenuation and distance-dependent spatial resolution (DDSR)) that adequate compensation for the effects of these physical factors requires data measured at projection angles over 2π . However, as the analysis below suggests, it appears possible that (at least under certain conditions) data acquired only over π can be used for adequately correcting for the effects of some physical factors such as photon attenuation. The reduction of the scanning angle in SPECT imaging is desirable because it can reduce scanning time and thereby minimize patient-motion and other artifacts. Also, in certain cases (e.g., in cardiac SPECT), one can choose the scanning angular range for obtaining maximum numbers of photons [3, 4]. This work focuses on investigation of accurate image reconstruction in 3D SPECT from data that are acquired with parallel-beam

collimation only over π and that contain the effects of photon attenuation (either uniform or non-uniform) and DDSR. For simplicity, we refer to such a scanning configuration as the 3D short-scan SPECT.

II. MATHEMATICAL RATIONALES

A. Redundant Information and Reduction of Scanning Angle

In some tomographic imaging systems, the data measured over 2π contain redundant information. One example is measurement of the 2D Radon transform [5], $p(\xi, \phi)$, of a real function over 2π , where ξ is the detector bin index and ϕ is the measurement angle. Such measurements contain redundant information because, in the absence of noise and other inconsistencies, the measurements from conjugate views are mathematically identical, i.e.,

$$p(\xi, \phi) = p(-\xi, \phi + \pi). \quad (1)$$

It is well known that such information can be exploited for reducing the scanning angle from 2π to π because *the maximum difference between the values of the real angles on the two sides of Eq. (1) is π* .

In fan-beam computed tomography (CT), the quantity $q(t, \beta)$ is used to denote the measured transmission data, where t indicates the detector bin index and β the measurement angle. Although the fan-beam measurements (except for those with $t = 0$) from conjugate views are not mathematically identical, one can still show that the fan-beam data acquired over 2π contains redundant information, i.e.,

$$q(t, \beta) = q(-t, \beta + \pi + 2\alpha(t)), \quad (2)$$

where $\alpha(t)$ is a known and *real* function of t , and its explicit form depends upon the detector configurations [6, 7]. It can be shown that $\max\{2\alpha(t)\} = 2\alpha(t_{max})$, where t_{max} is a positive finite number and $|t| \leq t_{max}$. In most practical situations, $2\alpha(t_{max}) < \pi$. Therefore, *the maximum difference between the values of the real angles on the two sides of Eq. (2) is $\pi + 2\alpha(t_{max})$, which is less than 2π* . It is well known that such redundant information can be exploited for reducing the scanning angle from 2π to $\pi + 2\alpha(t_{max})$, which is referred to as the short-scan (or half-scan) fan-beam CT [8, 9].

In diffraction tomography (DT) [10, 11], one can derive a quantity $M(\nu, \phi)$ from the measured data at a particular angle ϕ , where ν can be interpreted as the spatial frequency of the measured data function. It has been shown that $M(\nu, \phi)$ measured at angles over 2π contains redundant information [12], i.e.,

$$M(\nu, \phi) = M(-\nu, \phi + \pi + 2\alpha(\nu)), \quad (3)$$

where $\alpha(\nu)$ is a known and *real* function of ν , and the explicit form of $\alpha(\nu)$ is determined by the DT scanning configurations. Also, it can be shown that $\max\{2\alpha(\nu)\} = 2\alpha(\nu_{max}) < \pi$, where ν_{max} is a positive finite number and $|\nu| \leq \nu_{max}$. Therefore, *the maximum difference between the values of real angles on the two sides of Eq. (3) is $\pi + 2\alpha(\nu_{max})$* , which is less than 2π . Again, such redundant information has been exploited for reducing the scanning angle from 2π to $\pi + 2\alpha(\nu_{max})$ in DT, which is referred to as the minimum-scan DT [13].

In summary, the data acquired over 2π in some tomographic imaging systems contain redundant information, which can be exploited for reducing the scanning angles and/or to reduce noise in the reconstructed image [12, 14, 15]. The above analysis suggests that, because the physical scanning angle must be real, the maximum scanning angles are determined by *the maximum differences between the values of the real angles on the two sides of the equations* that characterize the consistent conditions of (or, equivalently, the redundant information in) the data functions in these imaging systems.

B. Redundant Information and Possible Reduction of Scanning Angle in SPECT

Now we consider 3D SPECT with parallel beam projection. When the effects of photon attenuation and DDSR are considered, from the measured data one can obtain the so-called modified sinogram, which can be expressed readily as

$$m(\xi, \phi, z) = \int d\eta e^{-\int_0^\eta d\eta' \mu(\xi \hat{\theta}(\phi) + \eta' \hat{\theta}^\perp(\phi), z)} \times \iint d\xi' dz' a(\xi' \hat{\theta}(\phi) + \eta' \hat{\theta}^\perp(\phi), z') h(\xi - \xi', z - z'; \eta), \quad (4)$$

where ξ and z are the 2D detector indices, $a(x, y, z)$ is the 3D radioactivity-distribution function; $\hat{\theta}(\phi) = (\cos\phi, \sin\phi)$ and $\hat{\theta}^\perp(\phi) = (-\sin\phi, \cos\phi)$ are two orthogonal unit vectors; $x = \xi \cos\phi + \eta \sin\phi$; $y = -\xi \sin\phi + \eta \cos\phi$; $\mu(x, y, z)$ is the known 3D attenuation function; and $h(\xi, z; \eta)$ is the known distance-dependent spatial resolution function. The full-width-at-half-maximum (FWHM) of the latter function is dependent of the distance η . In this work, we consider $h(\xi, z; \eta)$ only as a shift-invariant resolution function. However, it can be a generally shift-variant resolution function.

1) Possible reduction of scanning angle in SPECT with uniform attenuation

Obviously, from inspection of Eq. (4) it is unclear whether the data acquired over $\phi \in [0, 2\pi)$ contain redundant information in 3D SPECT with the effects of non-uniform attenuation and a general DDSR. However, when only the effect of uniform attenuation is considered, the modified sinogram becomes the 3D exponential Radon transform (ERT) [16], and we have demonstrated previously that the 3D ERT acquired at $\phi \in [0, 2\pi)$ contain redundant information, i.e.,

$$M(\nu_m, \nu_z, \phi) = M(-\nu_m, \nu_z, \phi + \pi + \phi'(\nu_m)), \quad (5)$$

where $M(\nu_m, \nu_z, \phi)$ is the 2D Fourier transform of the modified sinogram $m(\xi, z, \phi)$ with respect to ξ and z , and where $\phi'(\nu_m)$

is a known and *purely imaginary* function of ν_m . We previously developed algorithms that exploit such redundant information for controlling noise in reconstructed SPECT images [14, 15, 17].

Can such redundant information in the ERT be exploited for reduction of the scanning angle? The analysis in Sec. II.A suggests that, because the physical scanning angle must be real, the maximum scanning angle is *the maximum difference between the values of real portions of the angles on the two sides of the equations* (e.g., see Eqs. (1-3) that characterize the redundant information.) In Eq. (5) of the ERT case, because $\phi'(\nu_m)$ is *purely imaginary*, we speculate that it may have no impact on the determination of the maximum physical scanning angle, which must be real, and thus that the ERT acquired only over $\phi \in [0, \pi)$ can be used for accurately reconstructing images in SPECT with uniform attenuation. Our numerical studies presented below seem to support our hypothesis strongly.

Furthermore, for SPECT with uniform attenuation and certain DDSR functions such as the Cauchy function [18, 19], one can show that the 2D Fourier transform of the modified sinogram satisfies Eq. (4). In this situation, $\phi'(\nu_m, \nu_z)$ becomes a function of ν_m and ν_z . However, most importantly, $\phi'(\nu_m, \nu_z)$ remains *purely imaginary*. Therefore, *the maximum difference between the values of the real angles on the two sides of Eq. (5) remains to be π* . This observation leads us to speculate that accurate images may be reconstructed from data acquired over π in SPECT with uniform attenuation and DDSR of certain forms. We investigated theoretically as well as numerically the image reconstruction from data acquired from only π in SPECT with uniform attenuation and DDSR. Indeed, our numerical investigation below suggests that the quality of images reconstructed from data acquired over π appear to be comparable to that of images reconstructed from data acquired over 2π .

2) Possible reduction of scanning angle in SPECT with non-uniform attenuation

So far, it has been generally believed that one needs data over 2π for accurate image reconstruction in SPECT with non-uniform attenuation. However, the seemingly promising numerical results below obtained for SPECT with uniform attenuation leads naturally to the question: Can accurate images be reconstructed from the data acquired only over π in SPECT with non-uniform attenuation? In an attempt to answer this question, we are currently conducting a theoretical investigation, which appears to be an exceedingly difficult task despite the fact that an analytic solution has recently been derived for full-scan SPECT with the effect of non-uniform attenuation [20, 21]. On the other hand, we also conducted numerical research on image reconstruction from data acquired over π in SPECT with non-uniform attenuation. These numerical results, which are presented in Sec. III below, indicate (at least for the cases that we studied) that the quality of images reconstructed from data acquired over π is comparable to that of images reconstructed from the data acquired over 2π in SPECT when attenuation is non-uniform.

We investigated numerically the image reconstruction from data acquired only at $\phi \in [0, \pi)$ in short-scan SPECT with the effects of both non-uniform attenuation and DDSR. Again, the results of these numerical studies, as shown below, seem to suggest that the quality of images reconstructed from data acquired over π appear to be comparable to that of images reconstructed from data acquired over 2π .

3) Reconstruction Algorithm

Although we speculate that one may need data acquired only over $\phi \in [0, \pi)$ for accurate image reconstruction in short-scan SPECT, it remains unclear whether “closed-form” algorithms can be derived to accomplish such reconstruction tasks. On the other hand, one may use iterative algorithms to reconstruct images (i.e., to obtain solutions $a(\vec{r})$ in Eq. (4)) from knowledge of the data $m(\xi, \phi, z)$ over $\phi \in [0, \pi)$. Additive iterative algorithms can be devised for obtaining the solution in Eq. (4). An important question is whether such algorithms converge and, if so, whether they converge uniquely to the correct solution. It may be possible to prove the convergence of such additive iterative algorithms in certain situations. However, for a data function that contains the effects of non-uniform attenuation and DDSR as shown in Eq. (4), it is generally difficult (if not impossible) to prove the convergence of additive iterative algorithms. More importantly, the additive iterative algorithms [22], in general, cannot guarantee the positivity of the solutions and thus can be susceptible to noise and other inconsistencies such as sample aliasing that always accompanies experimentally measured data.

For the purpose of simplicity, Eq. (4) can be rewritten symbolically as¹

$$g(y) = \int_{D_x} dx h(x, y) f(x) \quad \forall y \in D_y, \quad (6)$$

where the real and non-negative functions $g(y)$ and $f(x)$ denote the data and image functions with domains D_y and D_x , respectively, and $h(x, y)$ denotes the kernel of the imaging transformation, which, as shown in Eq. (4), is also non-negative. The task here is to find, from knowledge of the data $g(y)$ (or, equivalently, $m(\xi, \phi, z)$ over $\phi \in [0, \pi)$), a non-negative solution $f(x)$ (or, equivalently, $a(\vec{r})$) that satisfies Eq. (6) (or, equivalently, Eq. (4)). Because Eq. (6) (i.e., Eq. (4)) is an inherently non-negative integral equation, we propose to use the algorithm

$$f^{(n+1)}(x) = \frac{f^{(n)}(x)}{\int_{D_y} dy h(x, y)} \int_{D_y} dy \frac{h(x, y) g(y)}{\int_{D_x} dx h(x, y) f^{(n)}(x)} \quad (7)$$

to obtain the solution $f(x)$ (i.e., the image function $a(\vec{r})$), where n is the number of iterations.

The algorithm in Eq. (7) is related to the expectation maximization (EM) algorithm [23–27], which has been shown to yield the maximization-likelihood solution when the data

¹The symbols x and y here denote general 3D spatial coordinates in the image and data spaces, respectively, and should not be confused with the Cartesian coordinates x and y in Eq. (4).



Fig. 1: Representative slices of the activity map, superimposed on the attenuation maps.

function $g(y)$ contain Poisson noise [24]. Even in the absence of Poisson noise, from the perspective of solving the positive integral equation, it can be shown [28] that *the algorithm in Eq. (7) converges* in the sense that the Kullback-Leibler discrepancy between $f^{(n+1)}(x)$ and $f^{(n)}(x)$ approaches zero monotonically at a rate faster than $(\frac{1}{n})$. (Recall that it is generally difficult to prove the convergence of additive algorithms for Eq. (4).) If a unique solution to Eq. (7) exists, *one can show that $f^{(n+1)}(x)$ converges to that unique solution.*² Additionally, from a practical point of view, the algorithm in Eq. (7) is easy to implement because it involves only forward and backward transformations and, more importantly, guarantees the positivity of the solution. Numerical investigation suggests that the EM algorithm is generally less susceptible than additive algorithms to the unavoidable noise and inconsistencies contained in experimentally acquired SPECT data [22].

III. NUMERICAL RESULTS

We conducted computer simulation to evaluate the possibility of short-scan SPECT reconstruction, as we stipulated above. We considered a SPECT cardiac study. The 3D radioactivity map has a uniform concentration inside the myocardium and is zero elsewhere. The 3D attenuation map is non-uniform, with a value of 0.15 cm^{-1} inside the chest, except for the lungs, which have no attenuation. Representative slices of the radioactivity map, superimposed on the attenuation map, are shown in Fig. 1. For purposes of comparison, we also considered a uniform attenuation map that is obtained from the non-uniform one by removing the lungs. We used a Gaussian DDSR of the form $h(\xi, z; \eta) = \frac{1}{2\pi^2 \sigma_\eta^2} \exp\left\{-\frac{\xi^2 + z^2}{2\sigma_\eta^2}\right\}$ to model the blurring effect in the data, where the standard deviation $\sigma(\eta) = \sigma_0 + \sigma_1 \eta$ depends linearly upon the distance η . Noiseless SPECT projection data, covering the full 2π view, was generated with Poisson noise subsequently to produce noisy data. The simulated projection data consist of 120 views of 128 (radial) \times 32 (axial) sinograms with a bin size of $0.25 \times 0.25 \text{ cm}^2$. The simulated noisy 2π data have about ten thousand counts per slice.

In reconstruction, all the simulated views were used for producing “full-scan” reconstruction, whereas only half of the views, ranging from $\pi/2$ to $3\pi/2$, are used for generating “short-scan” reconstruction. Both modes of reconstruction generated $128 \times 128 \times 32$ images with a $0.25 \times 0.25 \times 0.25 \text{ cm}^3$ voxel size. In the results shown below, we considered three types of reconstructions: (a) EM reconstruction from the short-scan data over π ; (b) EM reconstruction from full-scan data over

²We are currently investigating the existence of the unique solution to Eq. (4) and the conditions under which the unique solution may exist.

2π ; and (c) FBP reconstruction from short-scan data over π .

Figure 2 shows representative slices of the images reconstructed from noiseless and noisy data, which contain only the effect of uniform attenuation. These results demonstrate qualitatively that, for both noiseless and noisy data, images reconstructed from the short-scan and full-scan data are of essentially similar quality. These reconstructions have effectively removed the effects of attenuation that can be clearly observed in the FBP reconstructions (in the form of reduced image brightness toward the center). Notice here that the total number of counts in the short-scan reconstruction is only half of that in the full-scan reconstruction. However, for a fixed scanning time, one would expect the short-scan data to have approximately the same number of counts as in the full-scan data. When this factor is taken into consideration, it would be interesting to compare quantitatively the noise properties between reconstructions from both short-scan and full-scan data, where the former have high signal-to-noise ratio than do the latter.

Figure 3 shows representative slices of the images reconstructed from noiseless and noisy data, which contain only the effect of non-uniform attenuation. Again, these results show that, for both noiseless and noisy data, images reconstructed from the short-scan and full-scan data are of comparable quality. These reconstructions have compensated effectively for the effects of attenuation that can be clearly observed in the FBP reconstructions. It is also interesting to note the differences in the attenuation artifacts in the FBP images between this and the above case.

We subsequently introduced the effect of a Gaussian DDSR, with $\sigma_0 = 0.2$ cm and $\sigma_1 = 0.02$, into the simulated data and repeated the studies above. Figure 4 displays representative slices of the images reconstructed from noiseless and noisy data, which contain the effects of both uniform attenuation and Gaussian DDSR. Again, these results suggest that, for both noiseless and noisy cases, images reconstructed from the short-scan and full-scan data are of comparable quality. These reconstructions have compensated effectively for the effects of uniform attenuation and DDSR, which can be clearly observed in the FBP reconstructions. Finally, Figure 5 displays representative slices of the images reconstructed from noiseless and noisy data, which contain the effects of both non-uniform attenuation and Gaussian DDSR. Again, these results indicate that, for both noiseless and noisy cases, images reconstructed from the short-scan and full-scan data have comparable quality and that the effects of non-uniform attenuation and DDSR have been compensated effectively for.

IV. CONCLUSIONS AND DISCUSSION

It has been observed that the redundant information contained in some tomographic imaging systems can be exploited for devising short-scan configurations in these imaging systems [8, 9, 13]. We have shown previously [14, 15, 17] that redundant information exists in data acquired over 2π in SPECT with uniform attenuation and DDSR of certain forms. These observations led us to hypothesize or speculate

that one may need data acquired over π instead of 2π for accurate image reconstruction in 3D SPECT, and thus to suggest the concept of short-scan SPECT. We propose the use of a non-linear EM algorithm to reconstruct images in short-scan SPECT. It can be shown that this EM algorithm converges, and that it converges to the unique solution if such a unique solution exists. We also performed a numerical investigation to verify and evaluate accurate image reconstruction in short-scan SPECT. These results indicate (at least for the examples studied) that the quality of the reconstructed images in short-scan 3D SPECT appears to be essentially similar to that of reconstructed images in full-scan 3D SPECT. We are currently performing a detailed quantitative evaluation of image quality and accuracy and will report its results in the near future.

We are also conducting a theoretical investigation on the possibility of obtaining analytical solutions in 3D short-scan SPECT when the effects of attenuation and DDSR are considered. Recent work [20, 21] on the analytical solutions for 2D full-scan SPECT with only the effect of non-uniform attenuation may provide useful insights into our investigation of short-scan SPECT. Investigations on such analytic solutions can be theoretically important in understanding the reconstruction problems in short-scan SPECT. For example, the existence of such an analytical solution³ will imply that the solution of Eq. (4) is unique, and consequently, that the non-linear iterative algorithm in Eq. (7) converges to the unique solution.

In this work, we discuss only the image reconstruction from data acquired at angles from 0 to π . In fact, this can be considered as a special case of the so-called *π -scheme short-scan SPECT* that we have proposed. Basically, in the *π -scheme short-scan SPECT*, the data can be acquired over disjointed angular intervals. We speculate that, as long as the summation of these intervals without conjugate views is larger than or equal to π , images with quality comparable to that of images in full-scan SPECT may be reconstructed. Our preliminary numerical investigation has confirmed this observation and suggests that reconstruction from data acquired over disjointed angular intervals converges even faster than that from data acquired from 0 to π in short-scan SPECT.⁴

This work is theoretically intriguing because it poses several theoretically interesting and challenging questions. Does a unique solution exist in 3D short-scan SPECT with the effects of attenuation and DDSR? If so, under what conditions does such a solution exist? Research intended to provide answers to these questions is currently under way. Also, the practical implications of this work seem to be significant because the proposed *π -scheme short-scan* allows data acquisitions at desired projection views at which the emitted gamma-rays may

³For instance, the Tretiak-Metz method is an analytic solution to the reconstruction problem in 2D full-scan SPECT with uniform attenuation. It is highly susceptible to data noise and inconsistencies. However, its existence guarantees that there is a unique solution to the inversion of the ERT from its knowledge over 2π .

⁴This is understandable because, from the numerical perspective, the linear transformation associated with data acquired over disjointed angular intervals generally is better conditioned than is that for data acquired from 0 to π in *π -scheme short-scan SPECT*.

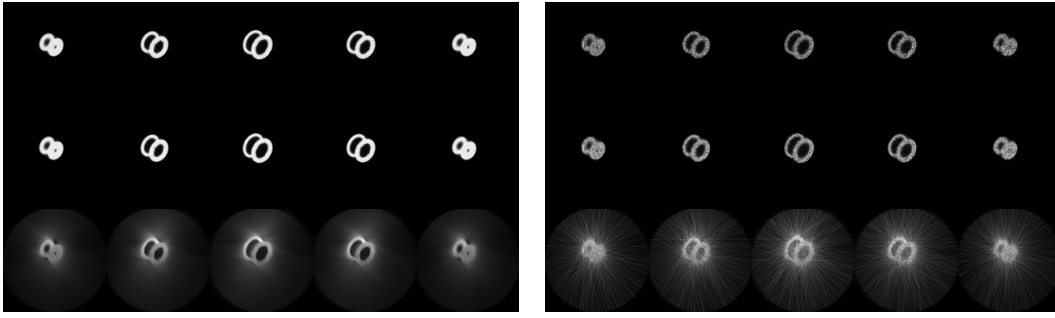


Fig. 2: Images reconstructed from simulated data with the only effect of uniform attenuation. Representative slices in the images reconstructed from noiseless (left panel) and noisy (right panel) short-scan data (1st row), the full-scan data (2nd row), and FBP reconstruction from short-scan data (3rd row). 50 and 20 iterations were used in the case of noiseless and noisy data, respectively, so that their total computation cost is identical.

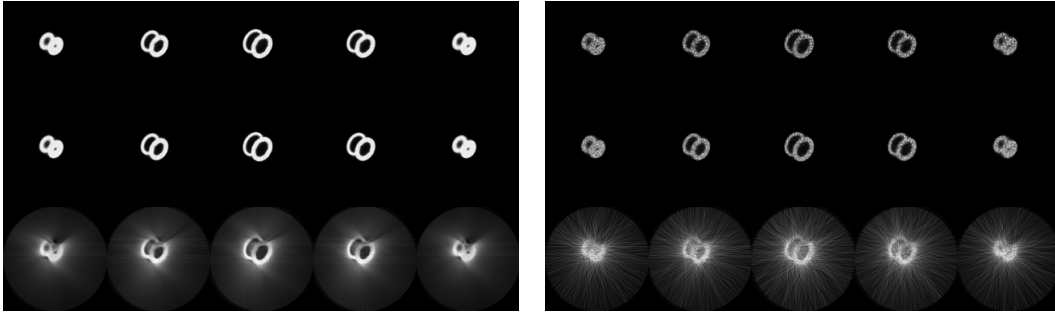


Fig. 3: Images reconstructed from simulated data with the only effect of non-uniform attenuation. Representative slices in the images reconstructed from noiseless (left panel) and noisy (right panel) short-scan data (1st row), the full-scan data (2nd row), and FBP reconstruction from short-scan data (3rd row). 50 and 20 iterations were used in the case of noiseless and noisy data, respectively.

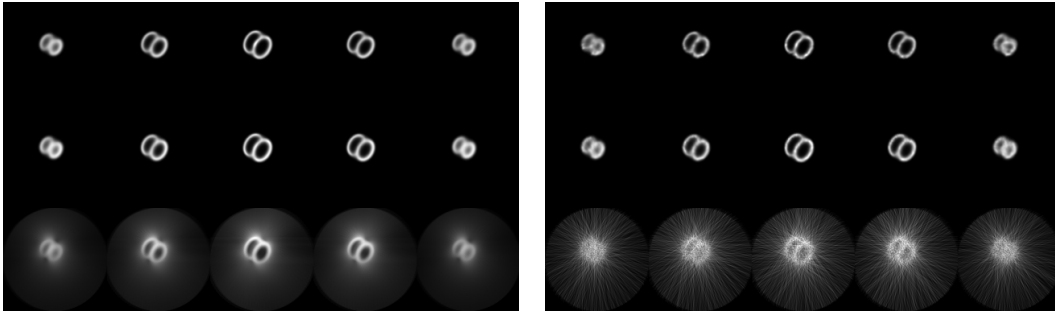


Fig. 4: Images reconstructed from simulated data with the effects of both uniform attenuation and DDSR. Representative slices in the images reconstructed from noiseless (left panel) and noisy (right panel) short-scan data (1st row), the full-scan data (2nd row), and FBP reconstruction from short-scan data (3rd row). 50 and 20 iterations were used in the case of noiseless and noisy data, respectively.

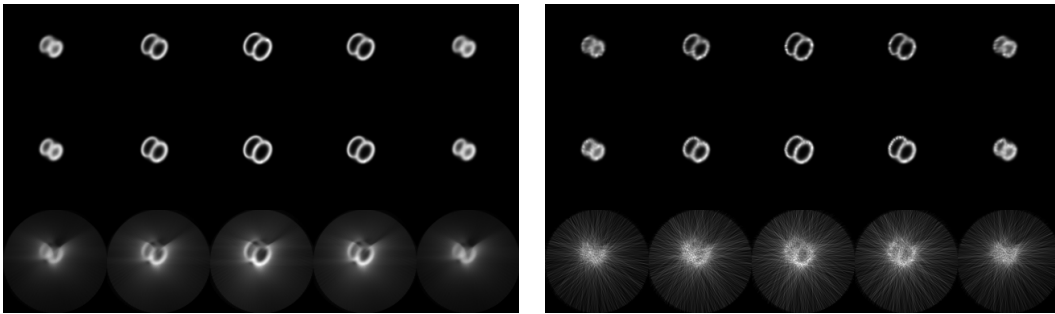


Fig. 5: Images reconstructed from simulated data with the effects of both non-uniform attenuation and DDSR. Representative slices in the images reconstructed from noiseless (left panel) and noisy (right panel) short-scan data (1st row), the full-scan data (2nd row), and FBP reconstruction from short-scan data (3rd row). 50 and 20 iterations were used in the case of noiseless and noisy data, respectively.

undergo the least attenuation and blurring, thus providing the freedom for significantly reducing the scanning time and for obtaining data with a high signal-to-noise ratio. One clinical study that may benefit from such a π -scheme scan is cardiac imaging with SPECT.

V. ACKNOWLEDGMENTS

This work was supported in part by National Cancer Institute Grants CA-70449 and CA-85593. Its contents are solely the responsibility of the authors and do not necessarily represent the official views of the National Cancer Institute.

VI. REFERENCES

- [1] T. F. Budinger, G. T. Gullberg, and R. H. Huesman. Emission computed tomography. In G. T. Herman, editor, *Image Reconstruction from Projections: Implementation and Application*, pages 147–246, Springer, New York, 1979.
- [2] R. J. Jaszczak, R. E. Coleman, and F. R. Whitehead. Physical factors affecting quantitative measurements using camera-based single-photon emission computed tomography (SPECT). *IEEE Trans. Nucl. Sci.*, 28:69–80, 1981.
- [3] R. T. Go, W. J. MacIntyre, T. S. Houser, M. Pantoja, D. H. F. J. K. O'Donnell, B. J. Sufka, D. A. Underwood, and T. F. Meaney. Clinical evaluation of 360° and 180° data sampling techniques for transaxial SPECT thallium-201 myocardial perfusion imaging. *J. Nucl. Med.*, 26:695–706, 1985.
- [4] K. Knesaurek, M. A. King, S. J. Glick, and B. C. Penney. Investigation of causes of geometrical distortion in 180° and 360° angular sampling in SPECT. *J. Nucl. Med.*, 30:1666–1675, 1989.
- [5] F. Natterer. *The Radon Transform*. Wiley and Sons, New York, 1986.
- [6] G. T. Herman. *Image Reconstruction from Projections*. Academic Press, New York, 1980.
- [7] A. Rosenfeld and A. C. Kak. *Digital Picture Processing*, volume 1. Academic Press, New York, 1982.
- [8] D. L. Parker. Optimal short scan convolution reconstruction for fan-beam CT. *Med. Phys.*, 9:245–257, 1982.
- [9] C. R. Crawford and K. King. Computed tomography scanning with simultaneous patient translations. *Med. Phys.*, 17:967–982, 1990.
- [10] R. Mueller, M. Kaveh, and G. Wade. Reconstructive tomography and applications to ultrasonics. *Proceedings of the IEEE*, 67:567–587, 1979.
- [11] S. Pan and A. Kak. A computational study of reconstruction algorithms for diffraction tomography: Interpolation versus filtered backpropagation. *IEEE Transactions on Acoustics, Speech, and Signal Processing*, 31:1262–1275, 1983.
- [12] X. Pan. A unified reconstruction theory for diffraction tomography with considerations of noise control. *J. Opt. Soc. Am.*, 15:2312–2326, 1998.
- [13] X. Pan and M. Anastasio. Minimum-scan filtered backpropagation algorithms in diffraction tomography. *J. Opt. Soc. Am.*, 16:2896–2903, 1999.
- [14] C. E. Metz and X. Pan. A unified analysis of exact methods of inverting the 2-D exponential Radon transform, with implications for noise control in SPECT. *IEEE Trans. Med. Imaging*, 14:643–658, 1995.
- [15] X. Pan and C. E. Metz. Analysis of noise properties of a class of exact methods of inverting the 2-D exponential Radon transform. *IEEE Trans. Med. Imaging*, 14:659–668, 1995.
- [16] O. J. Tretiak and C. E. Metz. The exponential Radon transform. *SIAM J. Appl. Math.*, 39:341–354, 1980.
- [17] X. Pan and C. E. Metz. Analytical approaches for image reconstruction in 3D SPECT. In P. Grangeat and J. Amans, editors, *3D Image Reconstruction in Radiology and Nuclear Medicine*, pages 103–116, Kluwer Academic Publishers, New York, 1996.
- [18] C. P. Appledorn. An analytical solution to the non-stationary reconstruction problem in single photon emission computed tomography. In D. A. Ortenhdahl and J. Llacer, editors, *Information Processing in Medical Imaging*, pages 69–79, Wiley-Liss, New York, 1990.
- [19] X. Pan. Analysis of 3D SPECT image reconstruction and its extension to ultrasonic diffraction tomography. *IEEE Trans. Nucl. Sci.*, 45:1308–1316, 1998.
- [20] R. G. Novikov. An inversion formula for the attenuated X-ray transformations. (preprint), 2000.
- [21] F. Natterer. Inversion of the attenuated Radon transform. (preprint), 2000.
- [22] B. M. W. Tsui, G. T. Gullberg, E. R. Edgerton, J. G. Ballard, J. R. Perry, W. H. McCartney, and J. Berg. Correction of non-uniform attenuation in cardiac SPECT imaging. *J. Nucl. Med.*, 30:497–507, 1989.
- [23] A. P. Dempster, N. M. Laird, and D. B. Rubin. Maximum likelihood from incomplete data via the EM algorithm. *JRSS*, 39:1–38, 1977.
- [24] L. A. Shepp and Y. Vardi. Maximum likelihood reconstruction for emission tomography. *IEEE Trans. Med. Imaging*, 1:113–122, 1982.
- [25] T. M. Cover. An algorithm for maximizing expected log investment return. *IEEE Trans. Information Theory*, 30:369–373, 1984.
- [26] I. Csizsár and G. Tusnády. Information geometry and alternating minimization procedures. *Statistics and Desisions*, Supplement issue 2:205–237, 1984.
- [27] K. Lang and R. Carson. EM reconstruction algorithms for emission and transmission tomography. *J. Comput. Assist. Tomogr.*, 8:306–318, 1984.
- [28] W. H. Wong. On Vardi's algorithm for positive integral equations. *Technical Report*, 334:1–12, Department of Statistics, The University of Chicago, 1991.